Results in Surfaces and Interfaces 19 (2025) 100535

Contents lists available at ScienceDirect

Results in Surfaces and Interfaces

journal homepage: www.elsevier.com/locate/rsurfi

Quartz crystal microbalance experiments reveal structural changes in the *Staphylococcus aureus* biofilm in the presence of savirin

Emilia M. Hudzik [a], Andrew J. Parnell [a], Jordan Petkov [b,c,*], Mark Geoghegan [a,d,**]

[a] School of Mathematical and Physical Sciences, The Hicks Building, The University of Sheffield, Hounsfield Road, Sheffield, S3 7RH, UK
[b] Arxada, Hexagon Tower, Blackley, Manchester, M9 8GQ, UK
[c] School of Physics and Astronomy, The University of Manchester, Schuster Building, Oxford Road, Manchester, M13 9PL, UK
[d] School of Engineering, Merz Court, Newcastle University, Newcastle-upon-Tyne, NE1 7RU, UK

ARTICLE INFO

Keywords:
Biofilm
Quorum sensing inhibitor
Staphylococcus aureus
Quartz-crystal microbalance

ABSTRACT

Quartz-crystal microbalance with dissipation (QCM-D) experiments show that green-fluorescent protein labelled *Staphylococcus aureus* adsorption to a gold QCM electrode is similar for a certain incubation period (here, 6 h) in the presence and absence of the quorum sensing inhibitor, savirin. After this period, cells continue to adsorb in the absence of savirin, but in its presence biofilm formation is severely compromised, with significant changes in the viscoelastic properties of the layer being observed.

1. Introduction

Biofilms are the epitome of how bacteria manifest their ability to exist in a high-density environment regulated by quorum sensing. The importance of biofilms in our everyday lives has been broadly discussed in the context, due to its detrimental effects, of healthcare environments; e.g., in medical devices (e.g., prosthetic joints), where conditions may be created for bacterial infection that are connected with biofilm formation [1]. Biofilms can also be found elsewhere in the body, for example, in the upper respiratory tract, on the teeth, on colonic mucosa, or in the cardiovascular system [2]. Healthcare is just one example, but biofilms are also responsible for the bacterial build up in water towers as well as in natural aquatic systems [3].

Biofilm formation comprises multiple stages [4]. In a first stage, individual cells move towards a surface on which their initial adsorption is reversible. At this stage it is common to treat the bacteria as colloidal systems interacting with the surface through mechanisms described by DLVO theory [5]. Adhesion subsequently becomes irreversible before, finally, the cell wall undergoes physical changes as extracellular polymeric substances are produced to form a stabilizing matrix for the emergent biofilm [4,6].

In forming a biofilm, quorum sensing enables cells to coordinate their collective behaviour [7–9]. This ability operates via the secretion and detection of autoinducer molecules, which accumulate in a cell density-dependent manner [10]. Reaching a certain level of those molecules can cause the cell to start expressing, for example, specific biopolymers to build an extracellular polymer matrix, which would benefit the bacteria, depending on the presence or absence of neighbouring microorganisms.

Staphylococcus aureus is an opportunistic pathogen that is responsible for a significant number of chronic infections due to its ability to form biofilms on tissue and medical instruments [11,12]. Biofilms provide a first line of defence for the bacteria against antibiotic treatments as well as other mitigations. Their stability and ability to withstand otherwise deleterious environments mean that preventing biofilm formation is preferable to developing a means of their elimination. The accessory gene regulator (*agr*) is a central regulator in *S. aureus* pathogenicity. Studies have shown that *agr* up-regulates the production of many exoproteins, and down-regulates the synthesis of cell wall associated proteins during post-exponential and stationary growth phases [13,14].

Impairment of quorum sensing systems, via the use of quorum-sensing inhibitors, has been shown to reduce bacterial deposition and attachment to substrates [15]. There are a number of quorum sensing inhibitors that have been shown to disrupt the *Staphylococcus aureus agr* [16–19], although other regulators have been targeted [20]. There are four *agr* groups divided into amino acid polymorphs (AgrA, AgrB, AgrC, and AgrD), with binding to the AgrA site having been demonstrated with two related small molecule inhibitors [16,18]. Savirin (*S. aureus*

* Corresponding author. Arxada, Hexagon Tower, Blackley, Manchester, M9 8GQ, UK.
** Corresponding author. School of Engineering, Merz Court, Newcastle University, Newcastle-upon-Tyne, NE1 7RU, UK.
E-mail addresses: jordan.petkov@manchester.ac.uk (J. Petkov), mark.geoghegan@newcastle.ac.uk (M. Geoghegan).

https://doi.org/10.1016/j.rsurfi.2025.100535
Received 14 January 2025; Received in revised form 14 March 2025; Accepted 20 April 2025
Available online 21 April 2025

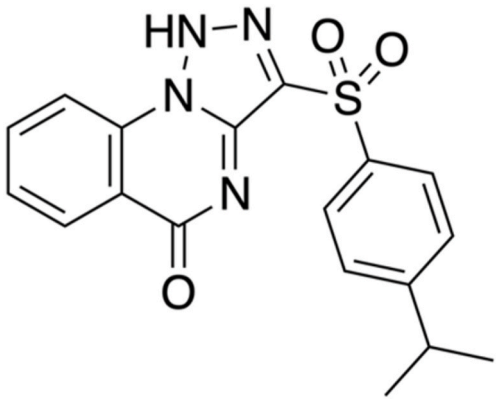

Fig. 1. Chemical structure of savirin.

virulence inhibitor, Fig. 1) is a small molecule inhibitor which disrupts *agr*-mediated quorum sensing by targeting AgrA [18].

In order to investigate the role of quorum sensing in biofilm formation, an experiment which aims to disrupt the signalling mechanism is presented here. Savirin, in particular, is known to target biofilm formation. Recent experiments have shown that savirin does inhibit biofilm formation in microtiter well plates [21]. In this work, savirin is used to interfere with biofilm growth in a green fluorescent protein (GFP) *S. aureus* biofilm on a gold quartz crystal microbalance electrode. To ensure that the microorganisms (GFP *S. aureus*) preserve their vitality during the experiment, a concentration well below the minimum biocidal concentration for savirin was chosen. It is shown that in the early stages of adsorption, adhesion is similar, but after ~6 h of growth, *S. aureus* adsorption behaviour diverges, with significant bacterial adsorption to the growing biofilm only occurring in the absence of savirin.

The detection of the cell threshold concentration at which the quorum sensing initiates is not a trivial task and to measure it one needs a technique with the sensitivity of a quartz crystal microbalance with dissipation (QCM-D) apparatus. Its ng/cm^2 resolution makes it a very attractive option for detecting the build-up of such networks of microorganisms surrounded by a polymer matrix. The method relies on gravimetrically measuring the mass of attached bacteria onto a gold crystal.

2. Experimental section

Protocol for bacterial growth. Green-fluorescent protein-labelled *S. aureus* (SH1000 GFP [22]) and a non-fluorescence control (American Type Culture Collection, ATCC 6538™ [23]) samples were kept as glycerol stocks at −80 °C. The bacteria were streaked on TSA (tryptone soy agar) plates and incubated for approximately 16 h at 37 °C. Single colonies from the plates were used to inoculate 3 mL of TSB (tryptone soy broth) and grown overnight (~16 h at 37 °C) under continuous shaking (200 rpm). The overnight cultures were then adjusted to an optical density, OD600 = 0.5 before use, using the corresponding media which was used in the initial growth step. SH1000 GFP includes a gene conferring resistance to the antibiotic tetracycline, 2 μg/mL of which was added to both the agar and broths used for GFP-labelled *S. aureus* growth. Savirin was stored at −80 °C at 500 μg/mL in DMSO before being added to the bacterial culture after the culture was diluted to OD600 = 0.5. Savirin was at a final concentration of 5 μg/mL, which is sufficiently dilute to retain the viability of the bacteria [21].

Quartz crystal microbalance with dissipation (QCM-D). Quartz crystal sensors (open QCM, Novaetech) with a fundamental frequency of 5 MHz were used in all QCM experiments. The electrodes consisted of 200 nm Au on 10 nm Ti substrate. The electrode diameter was 12 mm. The crystal cleaning procedure began with UV/ozone treatment (10 min). A 5:1:1 mixture of milliQ water, ammonia (25 %), and hydrogen peroxide (30 %) was heated to 75 °C in a fume hood. The sensor was placed in the solution and the temperature was maintained for 15 min. The sensor was rinsed with milliQ water immediately after removal from the solution. It was then dried using nitrogen gas and UV/ozone treated once more for 10 min. The sensors were used in experiments no later than 2 h following this cleaning protocol.

QCM experiments were conducted using the Q-Sense D300 (QSense, Biolin Scientific) system. The acquisition software, QSoft 301, and the analysing software, QTools, were used. The cleaning procedure began by inserting a designated cleaning sensor crystal into the chamber. Then, 2 % sodium dodecyl sulfate (SDS) was flowed through the loop and the chamber (30 mL flowed through each). The temperature of the system was increased to 40 °C and the SDS solution was left to sit in the chamber for 30 min to aid the cleaning process. Deionized (DI) water (40 mL) was then flushed through, followed by EtOH (30 mL) and finally DI water (10 mL). This three-step flushing procedure was then repeated. Residual DI water was removed from the system using nitrogen gas flow, then the cleaning crystal was removed, and the chamber area was dried. This cleaning protocol was conducted before and after each experiment.

Cleaned crystals were mounted into the QCM-D chamber, and the temperature set to 25 °C. Experiments began with loading the QCM with TSB for 20 min which allows for the stabilisation of the frequency and dissipation signals. Next, the overnight bacterial culture in TSB, adjusted to an OD at 600 nm of 0.5, was added to the chamber, displacing the liquid media. Both resonant frequency and dissipation values were recorded in real time. Data were collected for 24 h from the introduction of the bacteria into the system. After 24 h the buffer was flushed through the system, and data were recorded for a further 30 min. Three sets of

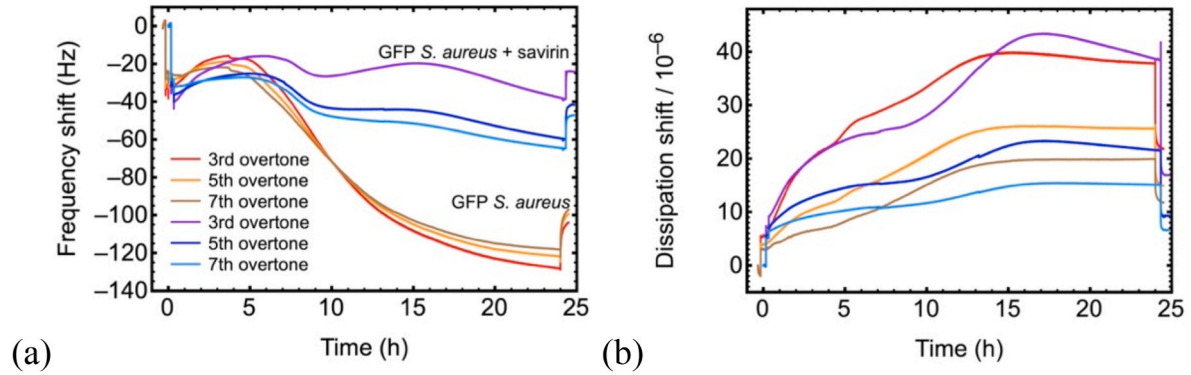

Fig. 2. Normalized Δ*f* (a) and Δ*D* (b) response of gold coated QCM sensor to GFP *S. aureus* in the presence and absence of savirin (5 μm/mL) in TSB. Bacteria are injected at 20 min, following a media-only background period. The dotted line at 30 min preceding the end of the experiment represents a PBS wash step. The legend in (a) applies also to the data in (b).

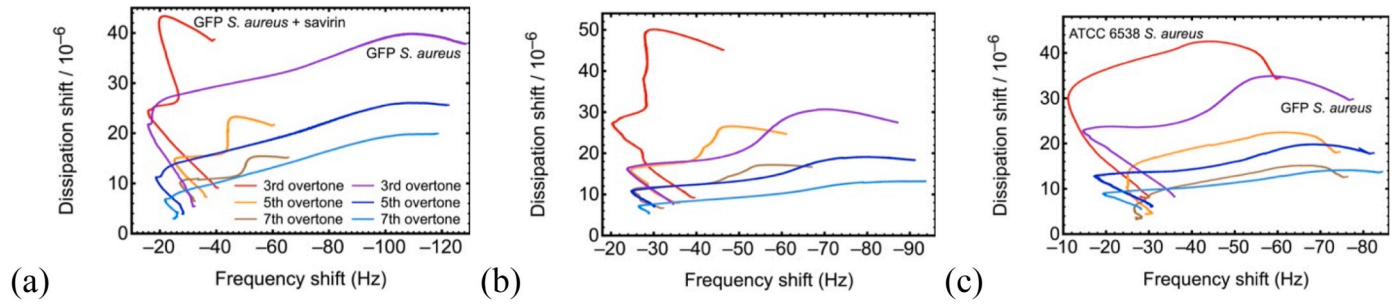

Fig. 3. Plots of Δf as a function of ΔD for the data shown in Fig. 2 (a) and a different data set (b). In (c) a different GFP *S. aureus* sample is compared with non-fluorescence ATCC6538 *S. aureus*, both in the absence of savarin. In all of these plots, the final wash and the initial bacterial injection periods are not shown. The legend included in (a) applies also to (b) and (c).

QCM experiments were each performed on GFP *S. aureus* in the presence of and without savirin, as well as on ATCC6538 *S. aureus*. All experiments demonstrated reproducibility, although one of the nine failed. Because a single channel QCM was used, these experiments were necessarily performed in series, which therefore required fresh bacterial cultures for each experiment, because the experimental time frame of >24 h is too long to use the same culture. This therefore offers further evidence of the robustness of the results and conclusions presented in this work. All of the QCM data are included in the supplementary material.

3. Results and discussion

Fig. 2 shows the results of two experiments: one in the presence of savirin, and one in its absence. In the first hour of cell adhesion the data show little difference with and without savirin (Fig. 2), which is unsurprising given that the low cell densities in this initial stage are unlikely to be sufficient for quorum sensing to be induced. The frequency data show two distinct QCM-D responses. Both plots show a peak in Δf within the first 5–7 h, but when savirin is absent, the frequency monotonically decreases, corresponding to increased bacterial adhesion. The experiment in the presence of savirin, in contrast, shows only small changes in frequency with time, which is expected to be due to the inhibition of quorum sensing upon reaching the cell density threshold level at about 6 h. The final Δf values reached at the end of the experiment differ by more than 60 Hz and reflect the role of the quorum sensing inhibitor in regulating the expression of extracellular polymeric substances. It has been shown elsewhere that *S. aureus* takes between 4 and 8 h before a biofilm forms and grows [24].

The dissipation data (Fig. 2b) for the samples with and without savirin are similar for the smallest overtone, $n = 3$, which typically indicates a similar level of viscoelasticity. However, the larger overtones do reveal a difference between the systems with and without savirin. These overtones are probing a shorter depth than that at $n = 3$ and suggest that the sample with savirin is more rigid than that without, which is consistent with the frequency shift data. The wash step at the end of the experiments shows similar effects in both data sets, with ΔD and the magnitude of Δf decreasing, indicating that adsorbed bacteria have been removed from the surface.

Although the frequency data (Fig. 2a) show clear differences with and without savirin, the differences for the dissipation data are harder to ascertain. With this in mind, adhesion fingerprints (plots of ΔD as a function of Δf) for the two situations are plotted in Fig. 3. In Fig. 3, the data for GFP *S. aureus* without savarin exhibit a slow increase in dissipation with increasing Δf, after the biofilm formation stage begins (6 h in Fig. 2a). This indicates cell spreading [25,26], which is complete towards the end of the experiment, corresponding to the largest Δf. When savirin is introduced to the medium, there are numerous changes in the stiffness of the cells (obtained from the slope of the adhesion fingerprint [26]), which indicates significant cytoskeletal organization within the experimental timeframe. The initial stages of biofilm formation are similar in these adhesion footprints, which indicates that savirin is ineffective until a critical point is reached in the coating of the gold electrode. Whilst there are significant differences in the data for GFP *S. aureus* in the presence and absence of savirin, these are much less pronounced when comparing GFP *S. aureus* to an ATCC 6538 *S. aureus* control, both in the absence of savirin.

The initial stage of bacterial adsorption is marked by decrease in (the absolute value of) Δf with time, which usually indicates a decrease in adsorbed mass. However, this conclusion does require that the Sauerbrey equation (describing adsorption in the QCM) holds, which, in turn, requires rigid adsorption. At the early stages of bacterial adsorption to a surface, adhesion is reversible and so this conclusion may not apply.

4. Conclusion

In this short communication, a study is presented covering the ability of GFP *S. aureus* to form a biofilm onto a molecularly smooth gold surface by means of QCM-D. It is observed that biofilm formation initiates between 5 and 7 h after the cells were introduced. It is believed that this is the time required to accumulate enough living cells for quorum sensing to be operative. The QCM-D data are reproducible and show the effect of savirin, a quorum sensing inhibitor specific for *S. aureus*. After ~6 h, attachment in the presence of savirin is severely compromised compared to the case when no savirin is present. More insight is obtained from adhesion fingerprint plots, which showed that the stiffness of the biofilm in the absence of savirin was largely constant, but that the behaviour of the nascent biofilm was characterized by a series of stages, which indicate a series of viscoelastic changes. These experiments show the sensitivity of QCM to quorum inhibition and indicate that quorum inhibition in GFP *S. aureus* is not significant in the early stages of bacterial adsorption.

CRediT authorship contribution statement

Emilia M. Hudzik: Writing – review & editing, Writing – original draft, Methodology, Investigation, Formal analysis. **Andrew J. Parnell:** Supervision, Project administration, Methodology. **Jordan Petkov:** Writing – review & editing, Writing – original draft, Supervision, Methodology, Funding acquisition, Conceptualization. **Mark Geoghegan:** Writing – review & editing, Writing – original draft, Supervision, Project administration, Funding acquisition, Formal analysis.

Declaration of competing interest

The authors declare that they have no known competing financial interests or personal relationships that could have appeared to influence the work reported in this paper.

Acknowledgements

The EPSRC is acknowledged for funding for a PhD scholarship for EH through the Centre for Doctoral Training in Polymers, Soft Matter, and Colloids (EP/L016281/1). We are grateful for further financial support from Arxada Ltd.

Appendix A. Supplementary data

Supplementary data to this article can be found online at https://doi.org/10.1016/j.rsurfi.2025.100535.

Data availability

All data are included in the supporting material.

References

[1] Ricciardi, B.F., Muthukrishnan, G., Masters, E., Ninomiya, M., Lee, C.C., Schwarz, E.M., 2018. *Staphylococcus aureus* evasion of host immunity in the setting of prosthetic joint infection: biofilm and beyond. Curr. Rev. Musculoskelet. Med. 11, 389–400.
[2] Perry, E.K., Tan, M.-W., 2023. Bacterial biofilms in the human body: prevalence and impacts on health and disease. Front. Cell. Infect. Microbiol. 13, 1237164.
[3] Erdei-Tombor, P., Kiskó, G., Taczman-Brückner, A., 2024. Biofilm formation in water distribution systems. Processes 12, 280.
[4] Carniello, V., Peterson, B.W., van der Mei, H.C., Busscher, H.J., 2018. Physico-chemistry from initial bacterial adhesion to surface-programmed biofilm growth. Adv. Colloid Interface Sci. 261, 1–14.
[5] Hermansson, M., 1999. The DLVO theory in microbial adhesion. Colloids Surf. B 14, 105–119.
[6] Schilcher, K., Horswill, A.R., 2020. Staphylococcal biofilm development: structure, regulation, and treatment strategies. Microbiol. Mol. Biol. Rev. 84, e00026-00019.
[7] Bassler, B.L., Losick, R., 2006. Bacterially speaking. Cell 125, 237–246.
[8] Davey, M.E., O'Toole, G.A., 2000. Microbial biofilms: from ecology to molecular genetics. Microbiol. Mol. Biol. Rev. 64, 847–867.
[9] Hall-Stoodley, L., Costerton, J.W., Stoodley, P., 2004. Bacterial biofilms: from the natural environment to infectious diseases. Nat. Rev. Microbiol. 2, 95–108.
[10] Nadell, C.D., Xavier, J.B., Levin, S.A., Foster, K.R., 2008. The evolution of quorum sensing in bacterial biofilms. PLoS Biol. 6, e14.
[11] Archer, N.K., Mazaitis, M.J., Costerton, J.W., Leid, J.G., Powers, M.E., Shirtliff, M. E., 2011. *Staphylococcus aureus* biofilms. Virulence 2, 445–459.
[12] Peng, Q., Tang, X., Dong, W., Sun, N., Yuan, W., 2022. A review of biofilm formation of *Staphylococcus aureus* and its regulation mechanism. Antibiotics 12, 12.
[13] Recsei, P., Kreiswirth, B., O'Reilly, M., Schlievert, P., Gruss, A., Novick, R.P., 1986. Regulation of exoprotein gene expression in *Staphylococcus aureus* by agr. Mol. Gen. Genet. 202, 58–61.
[14] Traber, K.E., Lee, E., Benson, S., Corrigan, R., Cantera, M., Shopsin, B., et al., 2016. agr function in clinical *Staphylococcus aureus* isolates. Microbiology 154, 2265–2274.
[15] Vanoyan, N., Walker, S.L., Gillor, O., Herzberg, M., 2010. Reduced bacterial deposition and attachment by quorum-sensing inhibitor 4-nitro-pyridine-*N*-oxide: the role of physicochemical effects. Langmuir 26, 12089–12094.
[16] Mahdally, N.H., George, R.F., Kashef, M.T., Al-Ghobashy, M., Murad, F.E., Attia, A. S., 2021. Staquorsin: a novel *Staphylococcus aureus* Agr-mediated quorum sensing inhibitor impairing virulence in vivo without notable resistance development. Front. Microbiol. 12, 700494.
[17] Murray, E.J., Crowley, R.C., Truman, A., Clarke, S.R., Cottam, J.A., Jadhav, G.P., et al., 2014. Targeting *Staphylococcus aureus* quorum sensing with nonpeptidic small molecule inhibitors. J. Med. Chem. 57, 2813–2819.
[18] Sully, E.K., Malachowa, N., Elmore, B.O., Alexander, S., Femling, J.K., Gray, B.M., et al., 2014. Selective chemical inhibition of agr quorum sensing in *Staphylococcus aureus* promotes host defense with minimal impact on resistance. PLoS Pathog. 10, e1004174.
[19] Tal-Gan, Y., Stacy, D.M., Foegen, M.K., Koenig, D.W., Blackwell, H.E., 2013. Highly potent inhibitors of quorum sensing in Staphylococcus aureus revealed through a systematic synthetic study of the group-III autoinducing peptide. J. Am. Chem. Soc. 135, 7869–7882.
[20] Balamurugan, P., Praveen Krishna, V., Bharath, D., Lavanya, R., Vairaprakash, P., Adline Princy, S., 2017. *Staphylococcus aureus* quorum regulator SarA targeted compound, 2-[(methylamino)methyl]phenol inhibits biofilm and down-regulates virulence genes. Front. Microbiol. 8, 1290.
[21] Pant, N., Miranda-Hernandez, S., Rush, C., Warner, J., Eisen, D.P., 2022. Effect of savirin in the prevention of biofilm-related *Staphylococcus aureus* prosthetic joint infection. Front. Pharmacol. 13, 989417.
[22] Horsburgh, M.J., Aish, J.L., White, I.J., Shaw, L., Lithgow, J.K., Foster, S.J., 2002. σ^B Modulates virulence determinant expression and stress resistance: characterization of a functional rsbU strain derived from *Staphylococcus aureus* 8325-4. J. Bacteriol. 184, 5457–5467.
[23] Makarova, O., Johnston, P., Walther, B., Rolff, J., Roesler, U., 2017. Complete genome sequence of the disinfectant susceptibility testing reference strain *Staphylococcus aureus* subsp. *aureus* ATCC 6538. Genome Announc. 5, e00293-00217.
[24] Salazar, J., Amer, M.-À., Turó, A., Castro, N., Navarro, M., Soto, S., et al., 2023. Real-time detection of the bacterial biofilm formation stages using QCM-based sensors. Chemosensors 11, 68.
[25] Watarai, E., Matsuno, R., Konno, T., Ishihara, K., Takai, M., 2012. QCM-D analysis of material–cell interactions targeting a single cell during initial cell attachment. Sens. Actuators B 171–172, 1297–1302.
[26] Yongabi, D., Khorshid, M., Gennaro, A., Jooken, S., Duwé, S., Deschaume, O., et al., 2020. QCM-D study of time-resolved cell adhesion and detachment: effect of surface free energy on eukaryotes and prokaryotes. ACS Appl. Mater. Interfaces 12, 18258–18272.